INSTITUTE OF PHYSICS PUBLISHING JOURNAL OF OPTICS A: PURE AND APPLIED OPTICS

J. Opt. A: Pure Appl. Opt. **7** (2005) S219–S229 doi:10.1088/1464-4258/7/2/029

Spectroscopic studies of liquid solutions of R6G laser dye and Ag nanoparticle aggregates

M A Noginov[1], M Vondrova[1,3], S M Williams[1], M Bahoura[1], V I Gavrilenko[1], S M Black[1], V P Drachev[2], V M Shalaev[2] and A Sykes[1]

[1] Center for Materials Research, Norfolk State University, Norfolk, VA 23504, USA
[2] Purdue University, West Lafayette, IN 47907, USA

Received 19 August 2004, accepted for publication 14 October 2004
Published 20 January 2005
Online at stacks.iop.org/JOptA/7/S219

Abstract

We have found that R6G laser dye in a concentration of 0.1 g l^{-1} mixed with a solution of aggregated silver nanoparticles exhibits a new emission band with a maximum at 612 nm. This band does not exist in pure dye of comparable concentration or in a mixture of dye with a solution of single silver nanoparticles. A qualitatively similar red-shifted emission band is observed in pure R6G dye at very high concentration (3.8 or 16.7 g l^{-1}). In both cases, no changes occur to the shapes of the absorption spectra of the dye.

We explain the observed spectral changes in terms of J-aggregates of R6G molecules whose formation is probable in the presence of Ag aggregates with a complicated surface structure and is much less likely in the case of adsorption of dye molecules on single Ag nanoparticles.

Alternatively, many features observed in the experiment can be explained by an enhancement of the rates of spontaneous radiative transitions in the proximity of metallic particles, which is due to a modification of the local density of electromagnetic modes in the vicinity of metal surfaces at energies resonant with surface plasmon resonances.

Keywords: laser dyes, aggregates of dye molecules, aggregates of silver nanoparticles, emission enhancement

1. Introduction

Metallic particles and rough metallic surfaces can strongly influence the optical responses of organic and inorganic materials. It has been demonstrated [1–4] that metals affect the shapes of absorption and emission spectra as well as the kinetics of luminescence decay. Enhancement of absorption and emission of Rhodamine 6G (R6G) and Nile Blue dyes on specially prepared metallic surfaces has been demonstrated by Glass *et al* in [1]. Changes in the optical properties of R6G dye molecules adsorbed on rough silver surfaces or in the presence of metallic nanoparticles have been also observed in [2, 5, 6]. In rare-earth doped materials, the effect of enhanced luminescence by silver islands has been demonstrated in Er^{3+}:sol–gel glasses [3].

Metallic particles and surfaces also strongly affect *nonlinear* responses of optical materials. The well-known examples include surface enhanced Raman scattering (SERS) and harmonic generation [6, 7]. Strong enhancements of nonlinear optical properties have been demonstrated when metallic nanoparticles form fractal-structured aggregates [6].

R6G dye molecules possess non-zero dipole electric moments, which play a key role in the optical response from molecular aggregates [8–10]. It has been shown [10] that optical absorption from H-type R6G aggregates (where molecules form perfect sandwich structures) is modified while the luminescence spectra remain unchanged. On the other hand, for J-type R6G aggregates (with perfect 'end-to-end'

[3] Present address: Princeton University, Princeton, NJ 08544, USA.

Figure 1. A transmission electron microscope (TEM) picture of the silver aggregate used in the experiments.

alignment of dipole moments), a new luminescence band of R6G located at 610 nm has been reported [9].

The above suggests that further understanding of the optical responses from complexes of R6G dye molecules and metallic nanoparticles requires detailed studies of both macroscopic optical field resonances and quantum chemical processes.

In this work, we present the results of experimental and theoretical studies of the effect of single and aggregated Ag nanoparticles on the spectroscopic properties of Rhodamine 6G dye. We show that at certain concentrations of Ag aggregate and R6G molecules in the mixture, an entirely new band appears in the emission spectrum of the dye which does not exist for pure R6G dye solution of comparable concentration. Equilibrium configurations and the electron energy structure of R6G single molecule and molecular aggregates absorbed on Ag surfaces are studied on the basis of first-principles modelling in the context of density functional theory (DFT).

2. Experimental samples and set-up

In the course of our experiments, we studied absorption, emission, and excitation spectra of R6G dye and aggregated Ag nanoparticles mixed in different concentrations. Similar measurements were performed in solutions of R6G dye mixed with single Ag nanoparticles, pure solvent without nanoparticles, and highly concentrated dye solutions.

In the preparation of Ag nanoparticles and aggregates, silver was reduced by a monomeric residue of polyvinylpyrrolidone (PVP) in ethanol solution of NaOH (1.2×10^{-3} M). The Ag particles were then aggregated with the addition of NaOH. The mean radius of the Ag particles was $R_0 \approx 6$ nm (± 1.5 nm). Most of the aggregates contained between 5 and 40 particles.

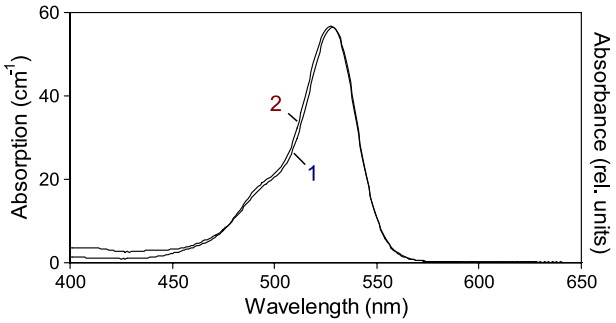

Figure 2. The absorbance spectrum of a droplet of highly concentrated R6G dye (3.8 g l^{-1}) placed between two microscope glass slides (1) scaled to fit the absorption spectrum of 0.1 g l^{-1} dye solution (2).

A transmission electron microscope (TEM) picture of one of the largest complexes (consisting of more than 40 aggregated silver nanoparticles) is shown in figure 1. The concentration of Ag particles was approximately 3.5×10^{13} cm^{-3}. Because of the relatively small sizes of the clusters of silver nanoparticles used in our experiments, the fractal dimension of the aggregate was difficult to estimate directly. It is known that aggregates of silver nanoparticles usually have a fractal dimension of 1.7–1.8 [11]. (As was shown by many groups [12], the fractal dimension can be introduced even for small clusters provided that there is a very large ensemble of clusters.)

Absorption spectra were studied when liquid samples were placed in 1 mm thick cuvettes using a Cary 5G UV–visible–IR spectrophotometer from Varian. When the concentration of dye was very high, a droplet of dye solution was placed between two glass slides. Emission and excitation spectra were studied using a FluoroMax-3 fluorometer from Jobin-Yvon.

In some measurements, samples were excited with $\approx$10 ns laser pulses at 532 nm. In this case, emission was focused at the entrance slit of an Oriel 257 monochromator, detected with a photomultiplier tube, and amplified and processed with a boxcar integrator.

The absorption (figure 2, trace 2), emission (figure 3, trace 1), and excitation spectra of a pure solution of R6G in methanol (0.1 g l^{-1}, the concentration recommended by Lambda Physik for dye lasers pumped at 0.53 μm), were very close to those previously reported in the literature [13].

3. Spectroscopic study of the mixture of R6G dye and Ag aggregate

3.1. Experimental procedure

In the course of the experiment, we first added a solution of Ag aggregates to a pure solution of R6G in methanol (0.1 g l^{-1}), continuously increasing the concentration of Ag particles and diluting the dye. Absorption, emission, and excitation spectra have been recorded at different concentrations of the mixture. After we reached the concentrations of dye and Ag aggregate at which the emission spectra of R6G changed significantly (figure 3), we diluted the mixture with pure solvent, reducing the concentrations of both dye and silver.

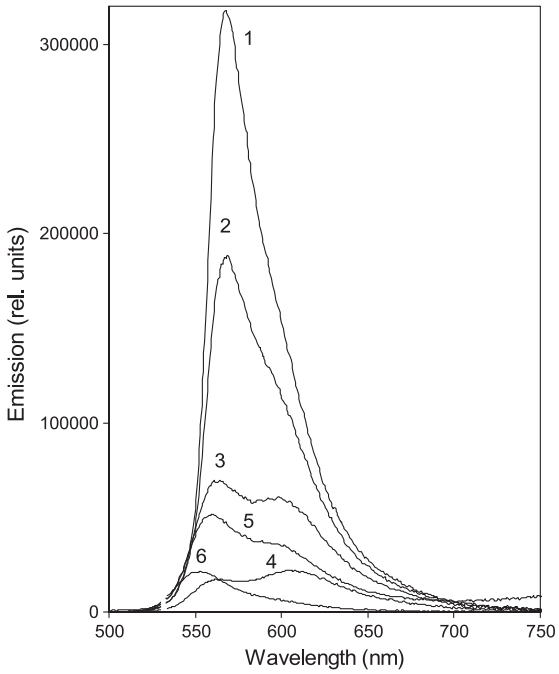

Figure 3. Emission spectra (with the dye excited at 0.53 μm in a 1 mm thick cuvette) of the mixtures of R6G and Ag aggregate. The concentrations of R6G and Ag aggregate in the mixtures are calculated as fractions of their maximum values in pure solutions (0.1 g l^{-1} and 3.5×10^{13} cm^{-3}, respectively). (1) $n_{R6G} = 1$, $n_{Ag} = 0$; (2) $n_{R6G} = 0.894$, $n_{Ag} = 0.106$; (3) $n_{R6G} = 0.620$, $n_{Ag} = 0.380$; (4) $n_{R6G} = 0.415$, $n_{Ag} = 0.585$; (5) $n_{R6G} = 0.189$, $n_{Ag} = 0.266$; (6) $n_{R6G} = 0.013$, $n_{Ag} = 0.019$.

3.2. Absorption spectra

The absorption spectrum of the mixture of R6G and Ag aggregate (figure 4, trace 2) can be fitted with the sum of the scaled absorption spectrum of pure Ag aggregate (figure 4, trace 3) and the scaled absorption spectrum of the pure dye (figure 2, trace 1). This suggests that the spectrum of the mixture does not have any features that do not belong to the absorption spectra of the constituents.

For each mixture, we determined the relative strength of R6G absorption and the relative strength of Ag absorption, defined as $\frac{k_{abs}^{R6G}}{k_{abs\ max}^{R6G}}$ and $\frac{k_{abs}^{Ag}}{k_{abs\ max}^{Ag}}$, respectively. (Here k_{abs}^{R6G} and k_{abs}^{Ag} are the absorption coefficients of the R6G dye and Ag aggregate measured at $\lambda = 530$ nm, and $k_{abs\ max}^{R6G}$ and $k_{abs\ max}^{Ag}$ are the corresponding *maximum* absorption coefficients measured in pure solutions.) In figure 5(a), the relative absorption of R6G in the mixture is plotted versus the relative concentration of R6G in the mixture defined as $\frac{n^{R6G}}{n_{max}^{R6G}}$, where n^{R6G} and n_{max}^{R6G} are, respectively, the dye concentrations in a given mixture and the initial pure R6G solution, 0.1 g l^{-1}. The experimental points in figure 5(a) follow the (expected) straight line at low R6G concentrations and deviate from a straight line (towards a reduction of R6G absorption) at high concentrations of dye.

The experimental curve in figure 5(a) (aggregate, triangles) can be fitted with high accuracy with an empirical formula

$$F_{R6G} = \frac{n^{R6G}}{n_{max}^{R6G}} - 3.4 \times \left(\frac{n^{R6G}}{n_{max}^{R6G}}\right)^4 \times \left(\frac{n^{Ag}}{n_{max}^{Ag}}\right), \qquad (1)$$

where n^{Ag} is the concentration of silver in a given mixture and n_{max}^{Ag} is its maximum concentration in the original Ag aggregate solution. This empirical description can be hypothetically interpreted as follows:

(i) some complexes, which involve aggregated silver nanoparticles and dye molecules in the proportion 1:4, are formed in the mixtures at high concentration of dye, and
(ii) the absorption of R6G molecules belonging to the complexes is strongly reduced in comparison with the absorption of single R6G molecules.

In figure 6, the relative absorption of Ag aggregate in the mixture is plotted versus relative R6G concentration $\frac{n^{R6G}}{n_{max}^{R6G}}$ (diamonds). A dashed line in figure 6 indicates the relative absorption of silver $\frac{k_{abs}^{Ag}}{k_{abs\ max}^{Ag}}$ which would be expected in the case of dilution of Ag aggregate by a solvent without dye. The measured experimental points match the dashed line at small concentrations of R6G and lie above it at high dye concentrations. The experimental dependence of $\frac{k_{abs}^{Ag}}{k_{abs\ max}^{Ag}}$ versus $\frac{n^{R6G}}{n_{max}^{R6G}}$ can be accurately fitted (figure 6, solid line) with an empirical formula

$$F_{Ag} = \left(\frac{n^{Ag}}{n_{max}^{Ag}}\right) + 3.9 \times \left(\frac{n^{R6G}}{n_{max}^{R6G}}\right)^4 \times \left(\frac{n^{Ag}}{n_{max}^{Ag}}\right), \qquad (2)$$

which contains exactly the same term $\left(\frac{n^{R6G}}{n_{max}^{R6G}}\right)^4 \times \left(\frac{n^{Ag}}{n_{max}^{Ag}}\right)$ as equation (1). This suggests that the same complexes as are responsible for reduced absorption of R6G in the mixture also lead to an increase in the absorption of aggregated silver nanoparticles.

Note that the high-accuracy fitting of the experimental curves in figures 5(a) and 6 cannot be accomplished using only combinations of 1:1, 2:1, and 3:1 complexes, but is readily possible when 4:1 complexes are taken into account. This indicates that 4:1 complexes give the predominant contribution to the anomalies in the concentration dependences depicted in figures 5(a) and 6. However, this does not exclude possible contributions from small concentrations of other complexes. The nature of the 4:1 complexes is the topic of future studies.

3.3. Emission spectra

The evolution of emission spectra in a series of mixtures with different concentrations of R6G and Ag aggregate are shown in figure 3. This figure presents the results of mixing the original R6G solution (0.1 g l^{-1}) with Ag aggregate and further dilution of the mixture with a pure solvent (methanol). With the increase of the concentration of Ag aggregate in the mixture, the second emission band, with the maximum $\lambda_{max} \sim 612$ nm, emerged in the spectrum. This is shown in more detail in figure 7, trace 1.

The 565 nm emission band of this spectrum can be fitted with reasonable accuracy to the scaled emission band of pure R6G dye of comparable concentration (see figure 7, trace 2). Trace 3 in figure 7, calculated as the difference between traces 1 and 2, can be interpreted as the spectrum of a new emitting centre. One can see that the new emission band (trace 3)

is broader than the original one (trace 2) and red-shifted by approximately 50 nm.

With the dilution of the mixture of R6G dye and Ag aggregate by pure solvent, the 612 nm emission band disappears and the emission spectrum returns nearly to its original shape, as can be seen by comparing traces 1 and 6 of figure 3. Thus, the formation of the new emitting centre, which can exist in a rather narrow range of R6G and Ag concentrations, is a reversible process.

3.4. Excitation spectra

In a pure R6G dye solution, the excitation spectrum of emission, recorded with the dye in a thin cuvette at a small concentration of dye, closely resembles the absorption spectrum. (When the two spectra are properly normalized, they are practically indistinguishable.)

In the mixture of R6G dye and Ag aggregate, the excitation spectrum of emission recorded at 567 nm (the original emission band of R6G) has the same shape as the excitation spectrum recorded at 600 nm (the new emission band), as shown in figure 4, traces 1a and 1b. Similarly, the shape of the emission spectrum does not depend on which of the two unresolved peaks in the excitation spectrum, 492 nm or 530 nm, is pumped (figure 4, traces 5a and 5b).

The shape of the excitation spectrum in figure 4 (traces 1a and 1b) approximately resembles that of the R6G absorption band in the mixture of R6G and Ag aggregate (trace 4, calculated as the difference between traces 2 and 3) and has nothing in common with the absorption spectrum of pure Ag aggregate (trace 3). No new excitation or absorption bands are observed in the mixtures in which the new emission band appears. Note that the difference between traces 1a, 1b and trace 4 was partially due to the relatively large optical thickness of the experimental sample.

Thus, we conclude that the luminescence of R6G in the mixture is most probably excited via direct pumping of dye molecules. We see no evidence of Ag-assisted excitation of R6G emission.

3.5. The concentration dependence of the emission intensity

Following the procedure discussed in section 3.3, all emission spectra of figure 3 were 'decomposed' into the sum of a regular emission band of R6G (with the maximum around 565 nm) and a new emission band (with the maximum around 612 nm). We then calculated the relative numbers of photons emitted in each band by evaluating the integrals $\int I(\lambda)\lambda\,\mathrm{d}\lambda$. Total emission signals were then calculated by adding the contributions from the 565 and 612 nm bands.

According to section 3.4, only photons which are directly absorbed by R6G molecules (or their complexes), contribute to the emission. Thus, we normalized the emission intensities calculated above by the relative numbers of photons absorbed by R6G and R6G-like centres in each particular mixture, $\left(\frac{k_{\mathrm{abs}}^{\mathrm{R6G}}(\lambda)}{k_{\mathrm{abs}}^{\mathrm{Ag}}(\lambda)}\right)\exp(-k_{\mathrm{abs}}^{\Sigma}(\lambda)l)$. (Here $l = 1$ mm is the thickness of the cuvette, and $k_{\mathrm{abs}}^{\Sigma}(\lambda)$, $k_{\mathrm{abs}}^{\mathrm{R6G}}(\lambda)$, $k_{\mathrm{abs}}^{\mathrm{Ag}}(\lambda)$ are, respectively, the total absorption coefficient of the mixture (at $\lambda = 0.53$ μm), the effective absorption coefficient of R6G and R6G-like centres, and the absorption coefficient of the Ag aggregate.) The resulting normalized emission intensities depicted in figure 8 can be interpreted as relative emission outputs per photon absorbed by R6G and R6G-like absorption centres in each mixture studied. The emission quantum yield in the initial solution of R6G dye was taken to be unity, which is close to the known experimental data [14, 15].

As one can see from figure 8, the relative total emission per photon absorbed by R6G and R6G-like centres approaches unity at low concentrations of Ag aggregate and is strongly reduced at high concentrations of Ag aggregate. This reduction in the emission quantum yield can be due to quenching of R6G luminescence in different complexes formed by R6G molecules and aggregated silver nanoparticles (this will be discussed in more detail in section 6).

3.6. Modelling of the concentration dependence of the emission and absorption

The purpose of this section is to show that the experimentally observed concentration dependence in the absorption and the emission of dye (figures 5 and 8) can be explained in terms of complexes formed by R6G molecules and silver nanoparticles. In real mixtures of dye and aggregated silver particles, a large number of different complexes can be formed simultaneously. Their detailed analysis can be very complicated and is not attempted here. Instead, we consider a model based on the assumption that there are only four species in the solution: 'unreacted' R6G, 'unreacted' Ag aggregate, 1:1 complexes (R6G)Ag, and 2:1 complexes $(\mathrm{R6G})_2\mathrm{Ag}$. We show that even this simple model can qualitatively describe the major trends in the experimental curves in figures 5 and 8.

The following equilibria then exist in our model solution:

$$\mathrm{R6G} + \mathrm{Ag} \xrightarrow{K_1} (\mathrm{R6G})\mathrm{Ag} \qquad \text{and} \tag{3}$$

$$2\mathrm{R6G} + \mathrm{Ag} \xrightarrow{K_2} (\mathrm{R6G})_2\mathrm{Ag}. \tag{4}$$

Here K_1 and K_2 are the equilibrium constants for reactions (3) and (4), respectively, defined as

$$K_1 = \frac{[(\mathrm{R6G})\mathrm{Ag}]}{[\mathrm{R6G}][\mathrm{Ag}]} \tag{5}$$

$$K_2 = \frac{[(\mathrm{R6G})_2\mathrm{Ag}]}{[\mathrm{R6G}]^2[\mathrm{Ag}]}, \tag{6}$$

where [ ] signifies the equilibrium concentration.

If R and A are the relative concentrations of R6G and Ag aggregate in the mixtures studied with respect to the concentrations of the original stock solutions, then

$$[\mathrm{R6G}] + [(\mathrm{R6G})\mathrm{Ag}] + 2[(\mathrm{R6G})_2\mathrm{Ag}] = R \qquad \text{and} \tag{7}$$

$$[\mathrm{Ag}] + [(\mathrm{R6G})\mathrm{Ag}] + [(\mathrm{R6G})_2\mathrm{Ag}] = A. \tag{8}$$

In order to fit the experimental curves with the solutions of equations (5)–(8), assumptions are made that

(i) the 2:1 complexes emit in the new band, with the maximum at 612 nm,
(ii) R6G molecules belonging to the 2:1 complexes have S-fold smaller absorption cross sections than regular dye molecules, and

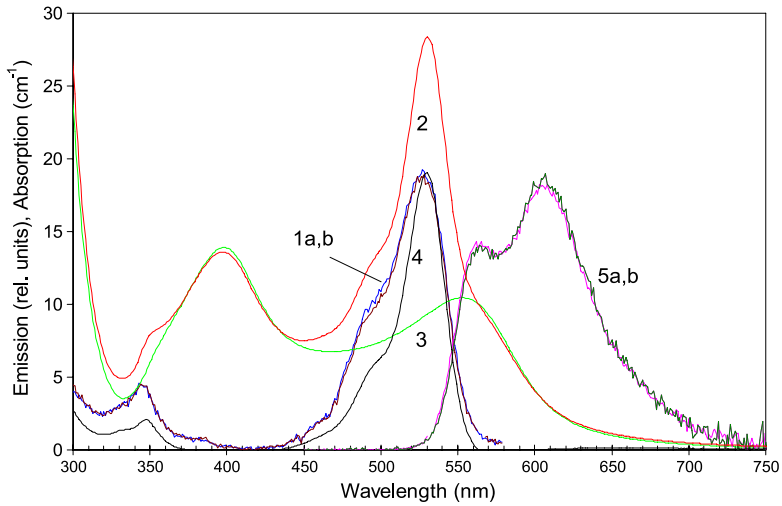

Figure 4. Traces 1a and 1b—excitation spectra of emission in the mixture of R6G and Ag aggregate; the emission was recorded at 567 nm (1a) and 600 nm (1b), and the two traces are scaled to fit each other. Trace 2—the absorption spectrum of the same mixture. Trace 3—the absorption spectrum of pure Ag aggregate of comparable concentration. Trace 4—the absorption spectrum of R6G in the mixture (calculated as the difference between traces 2 and 3). Traces 5a and 5b—emission spectra of the mixture of R6G and Ag aggregate; the emission was excited at 492 and 530 nm, respectively, and the two traces are scaled to fit each other. (The concentration of R6G in the mixture is equal to 42% of that in the original dye solution (0.1 g l^{-1}) and the concentration of silver in the mixture is equal to 92% of that in the original Ag aggregate solution.)

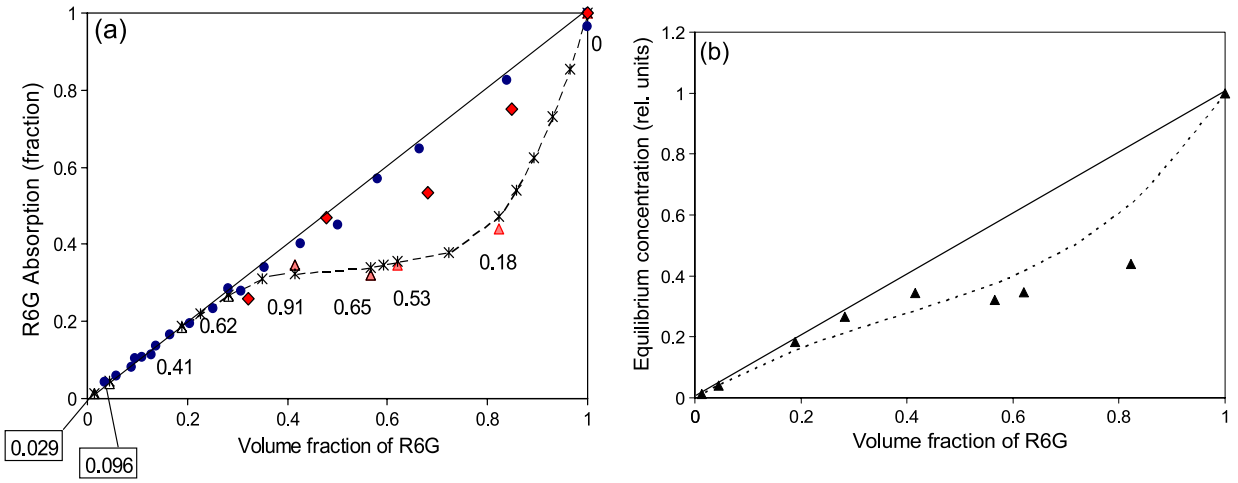

Figure 5. (a) The relative strength of R6G absorption (at 0.53 μm) plotted versus the relative R6G concentration. Triangles—experiment; dashed line with (⋇)—the fit with equation (1). Filled triangles correspond to the dilution of R6G dye with Ag aggregate and open triangles correspond to the further dilution with pure solvent. The relative concentration of Ag aggregate ($n^{\mathrm{Ag}}/n^{\mathrm{Ag}}_{\mathrm{max}}$, where n^{Ag} is the concentration of silver in a given mixture and $n^{\mathrm{Ag}}_{\mathrm{max}}$ is its maximum concentration in the original Ag aggregate solution) is indicated next to each point. Circles—the relative absorption of R6G diluted with pure solvent without silver nanoparticles. Diamonds—the relative absorption of R6G diluted with the solution of single silver nanoparticles. (b) The relative absorption of R6G at 0.53 μm (triangles, the same data as in (a)) fitted with the calculated function {[R6G] + [(R6G)Ag] + S[(R6G)$_2$Ag]}; section 3.6 (dashed curve).

(iii) R6G molecules belonging to the 1:1 complexes have the same absorption cross sections as regular dye molecules[4].

By varying the parameters K_1 and K_2, we fitted the relative intensity of the 612 nm emission band with the equilibrium concentration [(R6G)$_2$Ag] (figure 8(b)) and the relative absorption of dye at 530 nm with the sum {[R6G] + [(R6G)Ag] + S[(R6G)$_2$Ag]} (figure 5(b)).

[4] The first of these assumptions is in line with the discussion presented in section 6. The other two assumptions, whose justification requires a lot of spectroscopic studies and is beyond the scope of this paper, are also not unreasonable.

Considering the simplicity of the model, the fits which qualitatively describe the major features of the experimental curves and demonstrate the proof of principle of the proposed idea are quite reasonable. In order to get a more accurate fit, more complexes and more terms should be included in the model. For example, equation (1) and figures 5(a) and 6 suggest that 4:1 complexes should be taken into account.

4. Study of the mixture of R6G dye with single silver nanoparticles and solvent without nanoparticles

As discussed in section 3, the emission spectrum of R6G is changed strongly when dye is mixed with the solution of

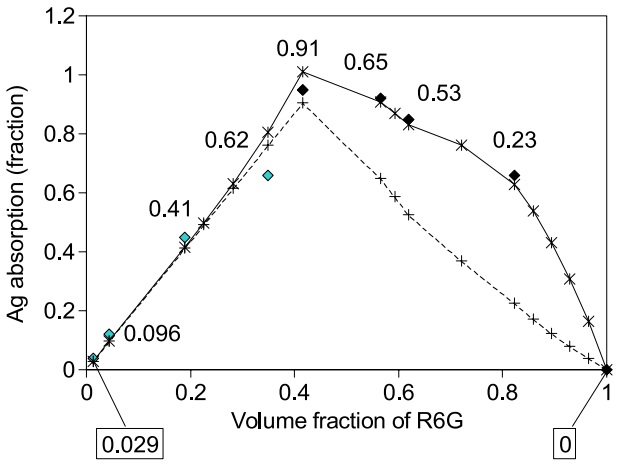

Figure 6. The relative absorption of Ag aggregate in the mixture plotted versus the relative R6G concentration. Diamonds—experiment; solid line with (✳)—the theoretical fit with equation (2). The relative concentration of Ag aggregate is indicated next to each point. Dashed line with (+)—the relative absorption of Ag aggregate which would be expected in the case of dilution of Ag aggregate by a solvent without dye.

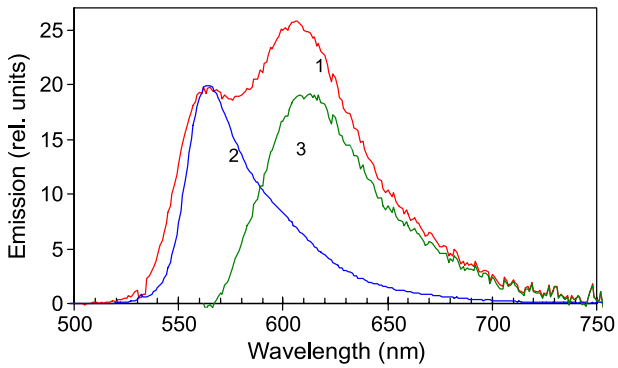

Figure 7. Trace 1—the emission spectrum of the mixture of R6G and Ag aggregate. (The concentration of R6G in the mixture is equal to 42% of that in the starting pure solution (0.1 g l^{-1}) and the concentration of Ag aggregate in the mixture is equal to 92% of that in the starting Ag aggregate solution.) Trace 2—the emission spectrum of the pure R6G of comparable concentration. Trace 3, the difference between traces 1 and 2, is the extracted spectrum of the new emission peak.

aggregated silver nanoparticles. The experiments described in this section were aimed at studying the effect of the solution of *single* (monomeric) silver nanoparticles and the *pure solvent*, which was used in section 3 to suspend silver nanoparticles, on the emission spectra of dye.

4.1. The effect of pure solvent

Diluting R6G dye first with an ethanol-based solvent containing PVP (the same solvent as was used to suspend the Ag aggregate in section 3) and then with pure methanol, we recorded a series of emission spectra demonstrating a slight but systematic change in the wavelength position of the emission maximum and the full width at half-maximum (FWHM) of the emission band; figure 9.

Qualitatively similar changes were detected in the absorption spectra. Following [8], we hypothesize that the observed slight changes of the spectra with the change of the dye concentration are due to the change of the polarity of the local environment of R6G molecules. In principle, the polarity depends both on the nature of the solvent and the dye concentration. In figure 9, the slopes of the lines fitted to experimental data points did not change significantly with the change of the solvent (ethanol-based or methanol). Thus we conclude that in this particular experiment the effect of dye concentration was stronger than the effect of solvent. At concentrations of R6G dye equal to or smaller than 0.1 g l^{-1}, we did not see in the spectra any signatures of dimers or other complexes of R6G molecules. These signatures have been observed in experiments with much higher concentrations of dye, which are discussed in section 5.

Upon the dilution of R6G with pure solvent, the absorption coefficient of dye decreased linearly with the decrease of the dye concentration (figure 5(a), circles) and the emission intensity per absorbed photon practically did not depend on the dye concentration (figure 8(a), open squares). This justifies asserting that the anomalous behaviours of the absorption (figure 5(a), triangles) and emission (figure 8(a), circles and diamonds) observed for mixtures of R6G and Ag aggregate, as well as the appearance of a new emission band (figures 3, 4, 7), are not merely due to the influence of the solvent.

4.2. The mixture of R6G with monomeric Ag nanoparticles

In this particular experiment, we studied the spectroscopic properties of the mixture of R6G dye with a solution of single (monomeric) Ag nanoparticles. The absorption spectra of the solutions of Ag monomer and Ag aggregate are shown in figure 10. The absorption band with a maximum at $\lambda \approx 0.4$ μm corresponds to the plasmon resonance in silver nanoparticles and the band with a maximum at $\lambda \approx 0.55$ μm (observed in Ag aggregate) corresponds to the interaction between nanoparticles. The two *integrated* absorption spectra had almost the same strength, $\int k_{\mathrm{abs}}^{\mathrm{aggregate}}\,[\mathrm{cm}^{-1}]\,\mathrm{d}E\,[\mathrm{cm}^{-1}] = 622\,[\mathrm{cm}^{-2}]$ for Ag aggregate and $\int k_{\mathrm{abs}}^{\mathrm{monomer}}\,[\mathrm{cm}^{-1}]\,\mathrm{d}E\,[\mathrm{cm}^{-1}] = 601\,[\mathrm{cm}^{-2}]$ for Ag monomer. Thus we concluded that the two solutions had about the same concentrations of silver. In the course of the experiment, we exactly followed the dilution routine described in section 3.1, the only difference being that single Ag nanoparticles were used instead of the Ag aggregate. The dependence of the relative absorption of R6G on the relative concentration of R6G in the mixture (figure 5(a), diamonds) is not a linear function as in the case of R6G diluted by pure solvent (figure 5(a), circles). However, the deviation from the linear dependence is not as strong as in the case of R6G diluted with Ag aggregate solution (figure 5(a), triangles).

The emission spectra of the mixtures of R6G and Ag nanoparticles are shown in figure 11. According to [13] and our study, absorption and emission spectra of pure R6G dye are composed of several bands corresponding to the transitions between different vibrational levels of the ground singlet state S_0 and the first excited singlet state S_1. This is why the emission spectrum of pure R6G dye has a very small shoulder at $\lambda \approx 0.59$ μm. When the solution of monomeric Ag nanoparticles is added to the dye solution, the relative strength of the shoulder is increased by a few per cent. The maximum wavelength of the addition to the shoulder, which could be due to the effect of

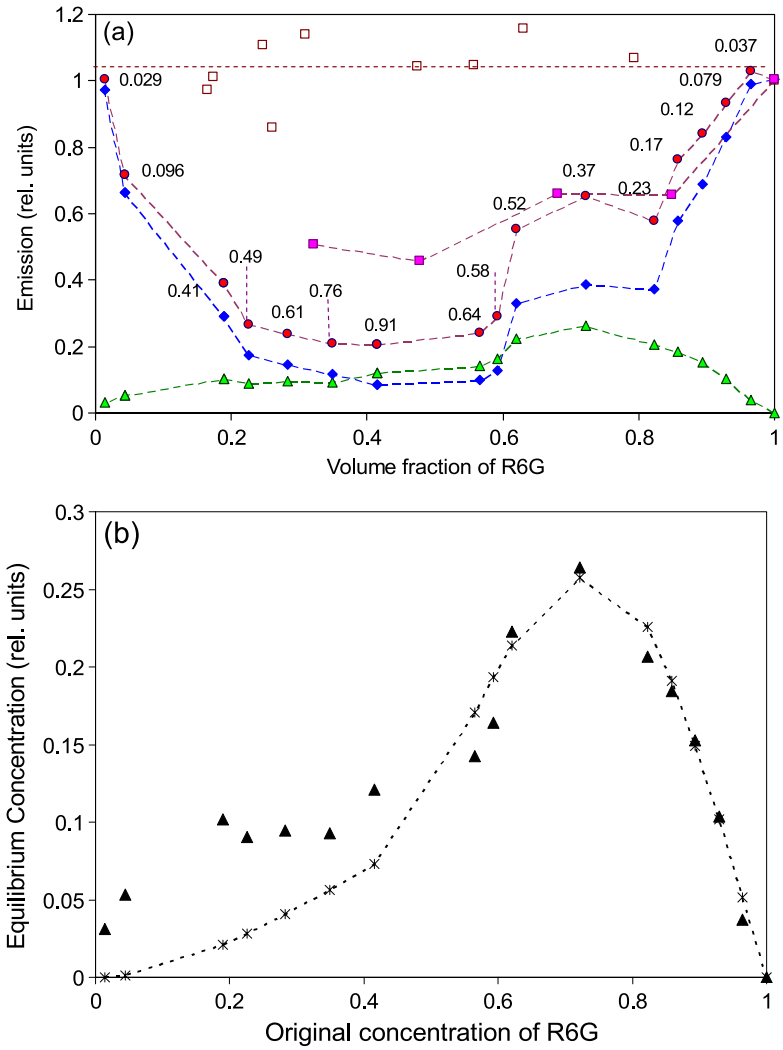

Figure 8. (a) Relative emission outputs in mixtures of R6G and Ag aggregate plotted versus n^{R6G}/n^{R6G}_{max}. Diamonds—the emission intensity of the 565 nm band; triangles—the emission intensity of the 612 nm band; circles—the sum of intensities of the 565 and 612 bands. Relative concentrations of Ag aggregate are shown next to the points. Open squares—the relative emission intensity in R6G diluted with the solvent without silver nanoparticles. Filled squares—the relative emission in R6G diluted with the solution of single silver nanoparticles. (b) The emission intensity of the 612 nm band (triangles—the same data as in (a)) fitted with the calculated equilibrium concentration $F[(R6G)_2Ag]$, section 3.6 (dashed curve with (⋇)).

monomeric Ag particles, was difficult to determine accurately. This very weak effect is much smaller than the effect of the Ag aggregate. When the dye solution was diluted with the solution of monomeric Ag nanoparticles, the total emission intensity decreased as well as the emission intensity per one absorbed photon (figure 8(a), filled squares). However, this effect was not as strong as in the case of R6G and aggregated silver nanoparticles. We speculate that with the addition of monomeric Ag solution to R6G, some complexes of dye molecules and silver nanoparticles are formed, as evidenced by the change of the absorption and emission intensity in figures 5(a) and 8(a). However, these complexes do not emit in the spectral band peaked at 612 nm.

5. Study of the emission and absorption of highly concentrated R6G dye

In the experiment described in this section, by increasing the concentration of dye we attempted to create complexes of R6G molecules (dimers or larger aggregates) and then examined their spectroscopic properties. The two dye solutions studied had concentrations of R6G equal to 3.8 and 16.7 g l^{-1}. The absorption of concentrated dye was so strong that it could not be studied with the dye in a standard 1 mm thick cuvette. The absorbance spectrum of a thin layer of dye (3.8 g l^{-1}) placed between two microscope glass slides is shown in figure 2. One can see that the shape of this absorbance spectrum is exactly the same as the shape of the absorption spectrum of R6G dye at a concentration of 0.1 g l^{-1}.

At the same time, the emission spectra of highly concentrated dyes are strongly different from that of dye at low concentrations; figure 12. The transformation of the emission spectrum with the increase of dye concentration qualitatively resembles the spectral transformation observed with the addition of Ag aggregate to the dye solution (compare figures 12 and 3). In both cases, the total intensity of emission decreases and the new, red-shifted emission band appears in the spectrum. When the emission spectrum splits into two bands,

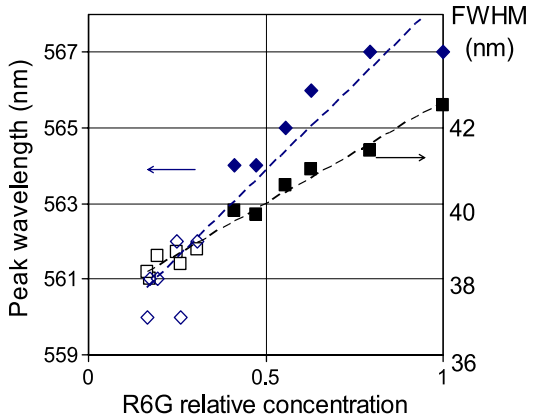

Figure 9. The wavelength of the maximum of the emission peak (diamonds) and the FWHM of the emission peak (squares) plotted against the relative concentration of R6G in pure solutions (without silver particles). Filled diamonds and squares correspond to initial dilution of R6G dye with the ethanol-based solvent; open diamonds and squares correspond to further dilution with pure methanol.

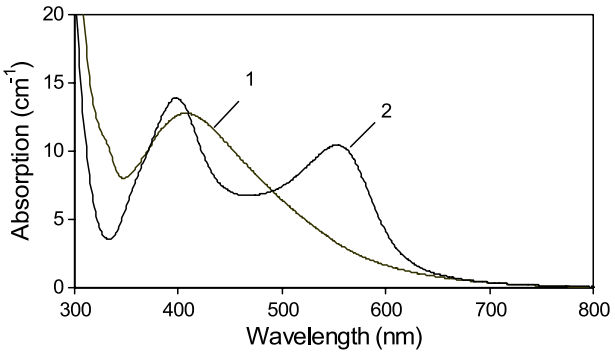

Figure 10. Absorption spectra of the solutions of single Ag nanoparticles (1) and Ag aggregate (2).

the position of the high-energy band in both cases remains close to the position of the emission band for pure low-concentration dye solution. However, the wavelength of the maximum of the red-shifted emission band for highly concentrated dye (602 nm at 16.7 g l^{-1} R6G concentration) is different from that for the mixture of dye and Ag aggregate (612 nm at $\leqslant$0.1 g l^{-1} R6G concentration). By combining the emission spectrum of dye with the transmission spectra corresponding to different dye concentrations, we have shown that the spectral shapes shown in figure 12 (traces 2 and 3) are not caused by absorption of dye. (Similarly, the shapes of the spectra in figure 3 are not due to the absorption of Ag aggregate.)

In the literature, spectral changes detected at high concentration of dye molecules, some of which resemble those observed in our experiments, are explained by the formation of aggregates of dye molecules [13]. This effect is discussed in more detail in section 6.

6. Discussion

Small shifts of the peak positions in the emission spectra of dyes are routinely caused by changes in the polarity of the environment [8]. We observed this effect when the R6G dye was diluted with a pure solvent or solutions of pure silver

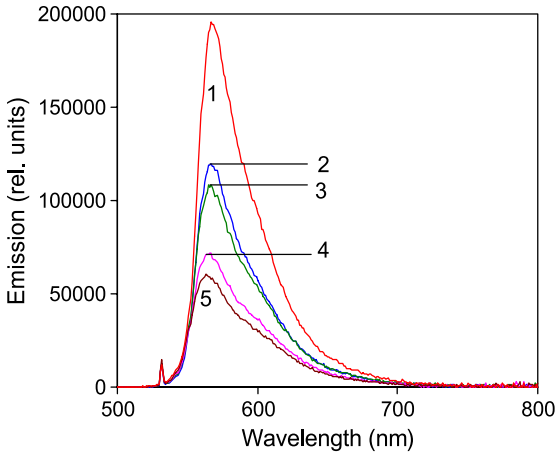

Figure 11. Emission spectra of R6G dye mixed with solutions of single silver nanoparticles. The concentrations of R6G and Ag monomer in the mixtures are calculated as fractions of their maximum values in the original solutions (equal to 0.1 g l^{-1} and 3.5×10^{13} cm^{-3}, respectively). (1) $n_{\mathrm{R6G}} = 1$, $n_{\mathrm{Ag}} = 0$; (2) $n_{\mathrm{R6G}} = 0.848$, $n_{\mathrm{Ag}} = 0.179$; (3) $n_{\mathrm{R6G}} = 0.680$, $n_{\mathrm{Ag}} = 0.202$; (4) $n_{\mathrm{R6G}} = 0.477$, $n_{\mathrm{Ag}} = 0.292$; (5) $n_{\mathrm{R6G}} = 0.321$, $n_{\mathrm{Ag}} = 0.196$. The emission was excited at 530 nm.

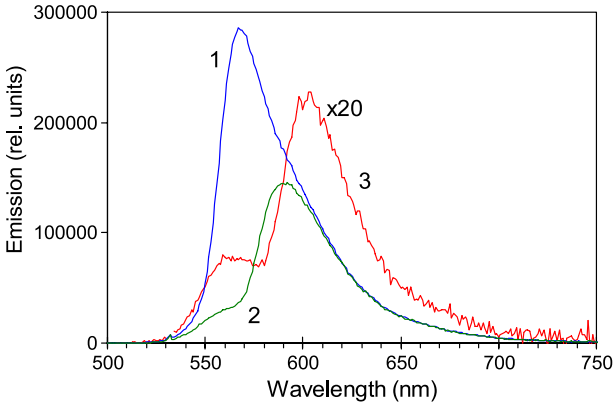

Figure 12. Emission spectra of pure solution of R6G in methanol at concentrations of dye equal to 0.1 g l^{-1} (1), 3.8 g l^{-1} (2), and 16.7 g l^{-1} (3). The emission intensity of trace 3 is 20-fold increased.

nanoparticles (figure 9). However, spectral shifts caused by the polarity are, as a rule, rather small and cannot explain the bimodal spectral shapes of figures 7 and 12.

According to [16], aggregation of the dye molecules leads to shifts of the state energies and splitting of the excited states. Depending on the mutual orientation of the molecules forming a dimer, different transitions in the system can be forbidden or allowed [8]. The optical properties associated with H-aggregates (when two molecules form a sandwich-like structure) and J-aggregates (with almost perfectly aligned dipole moments) of R6G molecules are extensively discussed in the literature [9, 10, 17] and references therein. It has been shown that J-type molecular aggregates result in the appearance of a new luminescence band at 610 nm [17], while H-type aggregates do not exhibit this effect [9, 17].

Assuming that the two emission bands seen in the spectra of figures 7 and 12 are due to splitting of the excited states of dimers, one can estimate the energy gap between the split states to be $\approx$1300 cm^{-1} for the mixture of R6G with Ag

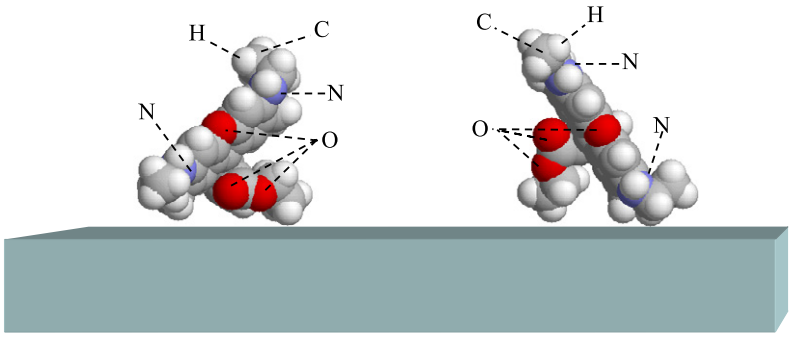

Figure 13. Geometries of Rhodamine 6G molecules adsorbed on Ag(111) predicted by the total energy minimization method. The colours of the balls correspond to different atoms: red (O), white (H), grey (C), blue (N).

aggregate and ≈1025 cm^{-1} for the highly concentrated pure dye. These values correspond to $6.2kT$ and $4.9kT$ at room temperature, where k is the Boltzmann constant and T is the temperature. At such large energy gaps, the Boltzmann population of the upper excited state would be very small and the corresponding luminescence negligible. Therefore, the two bands observed in the spectra of figures 7 and 13 most probably originate from emitting centres of at least two types: single R6G molecules and aggregates of dye molecules. The nature of the aggregates and the role of silver particles are discussed below. This scenario is in line with the heuristic equilibrium model presented in section 3.6.

The qualitative similarity of the spectra observed for highly concentrated dye (figure 12) and mixtures of dye with Ag aggregate (figure 7) suggests that the underlying physical mechanisms could be the same. We thus hypothesize that the significant spectral changes observed for the two system types are due to complexes of R6G molecules.

Geometry optimization of the R6G molecules was performed using a total energy minimization scheme [18]. The equilibrium geometry of the adsorbed R6G molecules on an Ag(111) surface is determined from the analysis of the total energy changes due to molecular adsorption. Density functional theory (DFT) was used as a basic method to evaluate the electron energy structure of the R6G molecule and the Ag(111) surface. The electron energy structure of the Ag(111) surface has been calculated using DFT with *ab initio* pseudopotentials of Ag generated as described in [19].

Analysis of the total energy changes shows two preferable configurations of R6G molecules on the Ag(111) surface (figure 13). In the two cases, the molecular axis creates an angle of ∼50° (left panel of figure 13) or ∼40° (right panel of figure 13) with the normal to the Ag(111) surface. It has been shown in the literature that when the angles between the longitudinal axes of Rhodamine molecules are smaller than 55°, J-aggregates are formed [17]. At the same time, larger angles result in the formation of (non-luminescent) H-type aggregates [17]. In order to study the effect of J-aggregation on luminescence spectra, we calculated the electron density structure of J-complexes modelled by two molecules aligned along their dipole moment directions. In our estimation, the distance between outer hydrogen atoms of two neighbouring molecules was equal to a typical intermolecular distance in organic crystals, 2.4 Å [20]. The *ab initio* DFT calculations of the orbital energies predict that J-type aggregation reduces the energy of a singlet–singlet transition by 0.09 eV (16 nm). This theoretical result is in qualitative agreement with the experimentally observed red-shift of the new emission band. The smallness of the predicted red-shift, in comparison with that observed experimentally, results from the restrictions of the model used, which will be optimized in future studies.

The geometry of the adsorbed R6G molecule (figure 13) suggests that H-type aggregates of R6G molecules can be created relatively easily on a silver surface, while J-type aggregates are not easily created. This calculation result is in agreement with the absence of a new emission band for the mixture of R6G dye and single silver nanoparticles. It is known that J-type R6G molecular aggregates showing a new luminescence band can be created on rough solid surfaces [17] or after intercalation [9]. Taking into account that Ag aggregates have very complex geometries, one can hypothesize that the probability of creating J-type R6G aggregates (resulting in the appearance of the 612 nm luminescence band) can be reasonably high.

Calculations to justify this conjecture as well as calculations of the energy levels of aggregated molecules are currently in progress. Qualitatively, we explain why the emission spectrum of aggregated R6G molecules is modified while the absorption spectrum is not in terms of a simplified configuration diagram, in which the configuration potential wells corresponding to the ground state and the excited state of a molecule are represented by quasi-parabolic curves; figure 14.

Let us assume that as a result of a perturbation (which could be due to the second molecule forming a dimer, for example), the position of the excited state potential changes as shown in figure 14 (‘slides’ along its wall). In this case, the position of the emission band can experience a red-shift without any shift in the energy of the absorption band. An example of a shifted potential curve can be found in [21]. (Note that in the schematic drawing of figure 14, the ‘system of coordinates’ is associated with the position of the potential well for the ground state.)

An alternative point of view has been proposed in [22–26], according to which, in proximity to metallic particles, the luminescent molecules or complexes experience

(i) an increase in the rate of spontaneous transition (due to modifications of the local density of electromagnetic modes in the vicinity of metal surfaces at energies resonant with surface plasmon resonances), and
(ii) luminescence quenching (due to energy transfer to a metal).

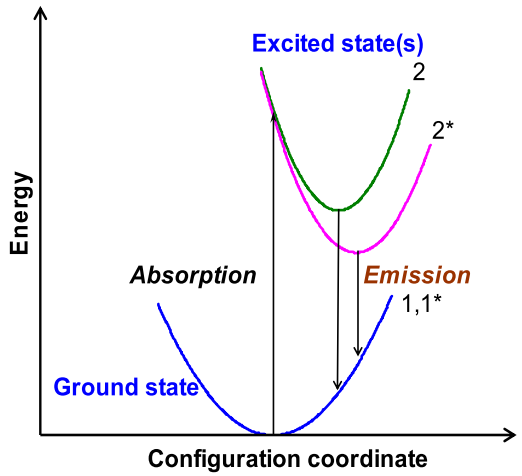

Figure 14. A simplified configuration energy diagram of a dye molecule. 1, 1*—the ground state of unperturbed and perturbed molecules; 2—the excited state of an unperturbed molecule; 2*—the excited state of a perturbed molecule. The perturbation is likely to be associated with the dimer formation.

With the increase in the distance d from the metal surface, the emission decay rate (dependent on the roughness of the surface) decreases as d^{-3} or faster [22], while the enhanced electric field decreases as $(R + d)^{-3}$, where R is the radius of the metallic particles. Hence, the optimum fluorescence occurs for molecules placed at a certain optimal distance from the surface [23–26]. It has been argued that as a result of the action of these two competing processes, the luminescence at relatively weak singlet–triplet transitions is enhanced and the luminescence at relatively strong singlet–singlet transitions is quenched. In principle, this model can explain many features observed in our experiments. First, the luminescence of the singlet–singlet transition with the maximum at ≈565 nm is suppressed in the presence of the Ag aggregate; figure 3. Second, the maximum of the new emission band at 612 nm (figure 7) approximately corresponds to the maximum of the triplet–singlet emission band of R6G molecules [27]. Third, the shape of the absorption spectrum for this mechanism of enhancement should not change, which is in agreement with our experimental result. However, without making additional assumptions this model does not explain

(i) the strong differences between the emission spectra of the mixtures containing Ag aggregates and the spectra of those with Ag monomers, and
(ii) the similarity between the spectra of the mixture of R6G and Ag aggregate and that of a highly concentrated solution of pure R6G dye.

7. Summary

We have found that R6G laser dye (in a concentration 0.1 g l^{-1}) mixed with a solution of aggregated silver nanoparticles exhibits a new emission band with a maximum at 612 nm, which does not exist for pure dye of comparable concentration or for a mixture of dye with a solution of single silver nanoparticles. A qualitatively similar red-shifted emission band is observed for pure R6G dye at very high concentration (3.8 or 16.7 g l^{-1}). In both cases, no changes occur in the absorption spectra of the dye.

We explain the observed spectral changes in terms of J-aggregates formed by R6G molecules. Equilibrium configurations and the electron energy structure of single R6G molecules and molecular aggregates absorbed on Ag surfaces have been calculated on the basis of first-principles modelling using the density functional theory (DFT). We conjecture that the formation of luminescent J-aggregates of R6G molecules is probable in the presence of Ag aggregates with complicated surface structures and is much less likely in the case of adsorption of dye molecules on single Ag nanoparticles.

Alternatively, many features observed in our experiments can be explained by an enhancement of the rates of spontaneous radiative transitions in the proximity of metallic particles, which is larger in the case of triplet–singlet transitions than in the case of singlet–singlet transitions. This enhancement is believed to be due to modifications of the local density of electromagnetic modes in the vicinity of metal surfaces at energies resonant with surface plasmon resonances.

Acknowledgments

This work was supported by the NASA grants NCC-1-01049 and NCC-3-1035 and the NSF grant HRD-0317722.

References

[1] Glass A M, Liao P F, Bergman J G and Olson D H 1980 Interaction of metal particles with adsorbed dye molecules: absorption and luminescence *Opt. Lett.* **5** 368–70
[2] Weitz D A, Garoff S, Gersten J I and Nitzan A 1983 The enhancement of Raman scattering, resonance Raman scattering, and fluorescence from molecules absorbed on a rough silver surface *J. Chem. Phys.* **78** 5324–38
[3] Selvan S T, Hayakawa T and Nogami M 1999 Remarkable influence of silver islands on the enhancement of fluorescence from Eu^{3+} ion-doped silica gels *J. Phys. Chem.* B **103** 7064–7
[4] Lakowicz J R, Gryczynski I, Shen Y, Malicka J and Gryczynski Z 2001 Intensified fluorescence *Photon. Spectra* (October 2001) 96–104
[5] Chandrasekharan N, Kamat P V, Hu J Q and Jones G II 2000 Dye-capped gold nanoclusters: photoinduced morphological changes in gold/Rhodamine 6G nanoassemblies *J. Phys. Chem.* B **104** 11103–9
[6] Shalaev V M 2000 *Nonlinear Optics of Random Media: Fractal Composites and Metal–Dielectric Films* (New York: Springer)
[7] Moskovits M 1985 Surface-enhanced spectroscopy *Rev. Mod. Phys.* **57** 783–826
[8] Kikteva T, Star D, Zhao Z, Baisley T L and Leach G W 1999 Molecular orientation, aggregation, and order in Rhodamine films at the fused silica/air interface *J. Phys. Chem.* B **103** 1124–33
[9] Sasai R, Iyi N, Fujita T, Arbeola F L, Martinez V M, Takagi K and Itoh H 2004 Luminescence properties of Rhodamine 6G intercalated in surfactant/clay hybrid thin solid films *Langmuir* **20** 4715–9
[10] Sasai R, Fujita T, Iyi N, Itoh H and Takagi K 2002 Aggregated structures of Rhodamine 6G intercalated in a fluor-taeniolite thin film *Langmuir* **18** 6578–83
[11] Drachev V P, Kim W-T, Safonov V P, Podolskiy V A, Zakovryashin N S, Khaliullin E N, Shalaev V M and Armstrong R L 2002 Low-threshold lasing and broad-band multiphoton-excited light emission from Ag aggregate–adsorbate complexes in microcavity *J. Mod. Opt.* **49** 645–62
[12] Jullien R and Botet R 1987 *Aggregation and Fractal Aggregates* (Singapore: World Scientific)

[13] Venkateswarlu P, George M C, Rao Y V, Jagannath H, Chakrapani G and Miahnahri A 1987 Transient excited state absorption in Rhodamine 6G *Pramana—J. Phys.* **28** 59–71
[14] Magde D, Wong R and Seybold P G 2002 Fluorescence quantum yields and their relation to lifetimes of Rhodamine 6G and fluoresce in nine solvents: improved absolute standards for quantum yields *Photochem. Photobiol.* **75** 327–34
[15] Kubin R F and Fletcher A N 1982 Fluorescence quantum yields of some Rhodamine dyes *J. Lumin.* **27** 455–62
[16] Pope M and Swenberg C 1982 *Electronic Processes in Organic Crystals* (Oxford: Oxford University Press)
[17] del Monte F and Levy D 1998 Formation of fluorescent Rhodamine B J-Dimers in sol–gel glasses induced by the adsorption geometry on the silica surface *J. Phys. Chem.* **102** 8036–41
[18] *Jaguar 4.0* 1991–2000 (Portland, OR: Schrödinger Inc.)
[19] Fuchs M and Scheffler M 1999 *Ab initio* pseudopotentials for electronic structure calculations of poly-atomic systems using density-functional theory *Comput. Phys. Commun.* **119** 67–98
[20] Davydov A S 1980 *Solid State Theory* (New York: Academic)
[21] Klessinger M and Michl J 1995 *Excited States and Photochemistry of Organic Molecules* (New York: VCH) p 547
[22] Arias J, Aravind P K and Metiu H 1982 The fluorescence lifetime of a molecule emitting near a surface with small, random roughness *Chem. Phys. Lett.* **85** 404
[23] Nitzan A and Brus L E 1981 Can photochemistry be enhanced on rough surfaces? *J. Chem. Phys.* **74** 5321–2
[24] Nitzan A and Brus L E 1981 Theoretical model for enhanced photochemistry on rough surfaces *J. Chem. Phys.* **75** 2205–14
[25] Wokaun A, Lutz H D, King A P, Wild U P and Ernst R R 1983 Energy transfer in surface enhanced luminescence *J. Chem. Phys.* **79** 509–14
[26] Mikhailovsky A, Ostrovski J and Bazan G C 2004 Surface plasmon enhanced organic light-emitting devices *Conf. on Lasers and Electro-optics* (paper #CWE1, CD ROM 2004 CLEO/IQEC Technical Digest, ISBN# 1-55752-770-9)
[27] Svelto O 1998 *Principles of Lasers* 4th edn (New York: Plenum)